

**EXPLOSION SOURCE MODELS FOR SEISMIC MONITORING AT HIGH FREQUENCIES:  
QUANTIFICATION OF THE DAMAGE SOURCE AND FURTHER VALIDATION OF MODELS**

Howard J. Patton

Los Alamos National Laboratory

Sponsored by the National Nuclear Security Administration

Award No. DE-AC52-06NA25396 / LA11-ExpSource-NDD02

**ABSTRACT**

This paper reports on the first year's accomplishments of a new project to extend explosion models, accounting for source medium damage, to high frequencies. This project builds on a previous three-year project which developed kinematic source descriptions for such models and investigated the seismic radiation for frequencies below  $\sim 0.2$  Hz. Direct and indirect effects of shock waves including free surface interactions cause material damage which in general contributes volumetric, compensated linear vector dipole (CLVD), and double-couple (DC) sources of seismic radiation. The past project studied two important features of these models: (i) Rayleigh waves excited by a CLVD source and the impact on performance of  $m_b$ - $M_s$  discrimination and (ii) volumetric moment caused by damage and its impact on estimates of isotropic moment  $M_I$  and yield estimation. The goal of the current project is to advance these models with a sound physical basis in order to study  $S$  wave generation for high frequencies. The tasking is broken down into three major phases: (1) develop and quantify mathematical descriptions of "effective" source functions for damage, which, up until now, were assumed to be a step function, (2) test and validate models against observed spectral features of  $P/S$  ratios for the 0.5-3 Hz band, and (3) test and validate models against scaling observations of  $P/S$  ratios for the 1-10 Hz band. This year's work involved empirical studies quantifying the amount of volumetric moment contributed by source medium damage. Quantification of  $M_I$  takes the form  $M_I \sim M_t \cdot K^x$ , where  $M_t$  is the classical moment due to cavity formation,  $K$  is a measure of damage tied to CLVD moment  $M_{clvd}$ , and exponent  $x$  is  $> 0$  for Pahute Mesa explosions (Patton and Taylor, 2011). For  $M_{clvd} = 0$ ,  $K = 1$ , and  $M_I = M_t$ . For a CLVD with permanent extensional deformation along the vertical axis,  $M_{clvd} > 0$ ,  $K > 1$ , and  $M_I > M_t$ , where excess volumetric moment is contributed by damage processes due to bulking and shear dilation of the source medium. The largest explosions on Pahute Mesa have  $K$  values of 1 or slightly less; thus, damage does not radiate much energy at long-periods, but it certainly can at high frequencies. At lower yields,  $K$  gets as large as 2.5 and  $M_I$  as much as 6 times  $M_t$ . I show results of modeling  $M_s$  scaling that exploit ground truth yields in order to place constraints on the value of  $x$ .

Increased understanding of the explosion source was applied to investigate source medium properties and  $m_b$  bias of the North Korean (NK) test site using yield : depth of burial tradeoff curves and  $\{m_b - M_s\}$  double differences (Patton, 2011). The results favor high  $P$  wave speeds, supporting the supposition that the granite medium in which NK tests were conducted is strong and intact. For the 2009 NK test, revised tradeoff curves accounting for better estimates of  $P$  wave speed and  $m_b$  bias predict yields of 7-8 kt for a burial depth of 550 m. This yield and burial depth give a scaled depth of  $\sim 300$  m/kt $^{1/3}$ . An emplacement scenario where NK tests were over-buried in competent granite supports previous claims that damage due to shock-wave interactions with the free surface was suppressed, leading to poor discrimination performance of  $m_b$  :  $M_s$  (Patton and Taylor, 2008). This work also validated our understanding that damage does not radiate energy effectively at long-periods for large Pahute Mesa explosions.

Finally, source specifications for numerical simulations of "effective"  $S$  wave source functions are being developed. These specifications quantify the damage distributed in depth from the free surface to the depth of burial. Effective source functions for  $S$  waves will be computed assuming direct generation and indirect generation through  $R_g$  scattering. A review of the specifications will be presented for discussion and comment.

<b>Report Documentation Page</b>		<i>Form Approved OMB No. 0704-0188</i>
Public reporting burden for the collection of information is estimated to average 1 hour per response, including the time for reviewing instructions, searching existing data sources, gathering and maintaining the data needed, and completing and reviewing the collection of information. Send comments regarding this burden estimate or any other aspect of this collection of information, including suggestions for reducing this burden, to Washington Headquarters Services, Directorate for Information Operations and Reports, 1215 Jefferson Davis Highway, Suite 1204, Arlington VA 22202-4302. Respondents should be aware that notwithstanding any other provision of law, no person shall be subject to a penalty for failing to comply with a collection of information if it does not display a currently valid OMB control number.		
1. REPORT DATE <b>SEP 2011</b>	2. REPORT TYPE	3. DATES COVERED <b>00-00-2011 to 00-00-2011</b>
4. TITLE AND SUBTITLE <b>Explosion Source Models for Seismic Monitoring at High Frequencies: Quantification of the Damage Source and Further Validation of Models</b>		
5a. CONTRACT NUMBER		
5b. GRANT NUMBER		
5c. PROGRAM ELEMENT NUMBER		
6. AUTHOR(S)		
5d. PROJECT NUMBER		
5e. TASK NUMBER		
5f. WORK UNIT NUMBER		
7. PERFORMING ORGANIZATION NAME(S) AND ADDRESS(ES) <b>Los Alamos National Laboratory,P.O. Box 1663 ,Los Alamos,NM,87545</b>		
8. PERFORMING ORGANIZATION REPORT NUMBER		
9. SPONSORING/MONITORING AGENCY NAME(S) AND ADDRESS(ES)		
10. SPONSOR/MONITOR'S ACRONYM(S)		
11. SPONSOR/MONITOR'S REPORT NUMBER(S)		
12. DISTRIBUTION/AVAILABILITY STATEMENT <b>Approved for public release; distribution unlimited</b>		
13. SUPPLEMENTARY NOTES <b>Published in the Proceedings of the 2011 Monitoring Research Review - Ground-Based Nuclear Explosion Monitoring Technologies, 13-15 September 2011, Tucson, AZ. Volume I. Sponsored by the Air Force Research Laboratory (AFRL) and the National Nuclear Security Administration (NNSA). U.S. Government or Federal Rights License</b>		

14. ABSTRACT

This paper reports on the first year's accomplishments of a new project to extend explosion models, accounting for source medium damage, to high frequencies. This project builds on a previous three-year project which developed kinematic source descriptions for such models and investigated the seismic radiation for frequencies below ~0.2 Hz. Direct and indirect effects of shock waves including free surface interactions cause material damage which in general contributes volumetric, compensated linear vector dipole (CLVD), and double-couple (DC) sources of seismic radiation. The past project studied two important features of these models: (i) Rayleigh waves excited by a CLVD source and the impact on performance of mb-Ms discrimination and (ii) volumetric moment caused by damage and its impact on estimates of isotropic moment MI and yield estimation. The goal of the current project is to advance these models with a sound physical basis in order to study S wave generation for high frequencies. The tasking is broken down into three major phases: (1) develop and quantify mathematical descriptions of ?effective? source functions for damage, which, up until now, were assumed to be a step function, (2) test and validate models against observed spectral features of P/S ratios for the 0.5-3 Hz band, and (3) test and validate models against scaling observations of P/S ratios for the 1-10 Hz band. This year's work involved empirical studies quantifying the amount of volumetric moment contributed by source medium damage. Quantification of MI takes the form  $MI \sim Mt \cdot K^x$ , where  $Mt$  is the classical moment due to cavity formation,  $K$  is a measure of damage tied to CLVD moment  $M_{CLVD}$ , and exponent  $x$  is  $> 0$  for Pahute Mesa explosions (Patton and Taylor, 2011). For  $M_{CLVD} = 0$ ,  $K = 1$ , and  $MI = Mt$ . For a CLVD with permanent extensional deformation along the vertical axis,  $M_{CLVD} > 0$ ,  $K > 1$ , and  $MI > Mt$ , where excess volumetric moment is contributed by damage processes due to bulking and shear dilation of the source medium. The largest explosions on Pahute Mesa have  $K$  values of 1 or slightly less; thus, damage does not radiated much energy at long periods but it certainly can at high frequencies. At lower yields,  $K$  gets as large as 2.5 and  $MI$  as much as 6 times  $Mt$ . I show results of modeling Ms scaling that exploit ground truth yields in order to place constraints on the value of  $x$ . Increased understanding of the explosion source was applied to investigate source medium properties and mb bias of the North Korean (NK) test site using yield : depth of burial tradeoff curves and {mb - Ms} double differences (Patton, 2011). The results favor high P wave speeds, supporting the supposition that the granite medium in which NK tests were conducted is strong and intact. For the 2009 NK test, revised tradeoff curves accounting for better

15. SUBJECT TERMS

16. SECURITY CLASSIFICATION OF:			17. LIMITATION OF ABSTRACT	18. NUMBER OF PAGES	19a. NAME OF RESPONSIBLE PERSON
a. REPORT unclassified	b. ABSTRACT unclassified	c. THIS PAGE unclassified	Same as Report (SAR)	11	

## **OBJECTIVE**

The objective is to develop new analytical explosion source models based on seismic moment tensor theory for further improvement and advancement of regional seismic discrimination and yield estimation technologies. Such technologies rely heavily upon the source information contained in high-frequency shear ( $S$ ) waves. The use of coda waves following regional  $S$  phases to estimate explosion yield is one example of an emerging technology offering great promise for improved nuclear monitoring. Unfortunately, an understanding of how explosions excite  $S$  waves is quite limited, and a widening gulf between theory and practice undermines our confidence to monitor broad areas at small yields. The new models will provide a physical basis for explosion-generated  $S$  waves and theoretical insights for advancing yield estimation and discrimination capabilities, thereby closing the gulf between theory and practice.

## **RESEARCH ACCOMPLISHED**

This project builds upon spherical (monopole) explosion source models developed in the 1970's. An important feature of those models is the theory relating seismic amplitudes of  $P$  waves directly to yield, depth of burial, and material properties of the source medium. The theory draws upon empirical yield scaling behaviors of key model constructs, such as the elastic radius, and the analytical nature of these models facilitated their use since they were easy to implement, and as such, widely applied to study the explosion source. Their application continues to this day, but with the recognition that a spherical point source is inadequate to explain  $S$ -wave generation.

The model under development consists of a monopole explosion source with linear superposition of tectonic and material damage sources. Material damage occurs as sudden changes in the source medium's elastic moduli. To date, our research has focused on long-period applications where all source components are safely assumed to be coincident in time and space, and share the same source-time histories. The current project will tackle high-frequency applications where those assumptions are no longer valid. Before doing so, certain key source parameters must be quantified, and among them is the isotropic or volumetric moment.

There are two sources of volumetric moment in the new source model, one from cavity formation and the other from damage processes (Patton and Taylor, 2011; hereafter PT11). Since tectonic release is modeled with a double-couple force system, it does not contribute volumetric moment. The moment tensor for a monopole explosion source is

$$M \cdot \begin{bmatrix} 1 & 0 & 0 \\ 0 & 1 & 0 \\ 0 & 0 & 1 \end{bmatrix}, \quad (1)$$

where  $M$  is a volumetric moment. Assuming an incompressible source medium,  $M = M_t$ , the moment due to cavity formation, where  $M_t = \rho\alpha^2 \cdot V_c$  ( $\rho$  and  $\alpha$  are density and  $P$  wave speed of the medium, and  $V_c$  is cavity volume; Mueller and Murphy, 1971; hereafter MM71).  $V_c$  can be calculated from cavity radius scaling models (e.g., Heard and Ackerman, 1967; Denny and Johnson, 1991; hereafter referred to as HA67 and DJ91). The moment tensor for damage can be expressed as a vertical dipole force (Knopoff and Randall, 1970; Ben-Zion and Ampuero, 2009).

$$M_d \cdot \begin{bmatrix} 0 & 0 & 0 \\ 0 & 0 & 0 \\ 0 & 0 & z \end{bmatrix}, \quad (2)$$

where  $M_d$  is a positive number (as is  $M_t$  for an explosion),  $zM_d$  is the moment of the dipole force, and  $z$  is a function of a new source parameter  $K$ ,  $z = z(K)$ . Recall that  $K$  is defined in PT11 as

$$K \equiv \frac{2M_{zz}}{M_{xx} + M_{yy}}, \quad (3)$$

where  $M_{xx}$ ,  $M_{yy}$ ,  $M_{zz}$  are diagonal elements of the full moment tensor source. Decomposing the damage source,

$$M_d \cdot \begin{bmatrix} 0 & 0 & 0 \\ 0 & 0 & 0 \\ 0 & 0 & z \end{bmatrix} = \frac{zM_d}{3} \cdot \begin{bmatrix} 1 & 0 & 0 \\ 0 & 1 & 0 \\ 0 & 0 & 1 \end{bmatrix} + \frac{2zM_d}{3} \cdot \begin{bmatrix} -0.5 & 0 & 0 \\ 0 & -0.5 & 0 \\ 0 & 0 & 1 \end{bmatrix}. \quad (4)$$

The second term on the right is a compensated linear vector dipole (CLVD) with moment  $2zM_d/3$  and vertical axis of symmetry in extension if  $z > 0$ . The net volumetric moment of explosion and damage sources is  $M_t + zM_d/3$ . The ratio of CLVD moment to net volumetric moment equals  $2zM_d/(3M_t + zM_d)$ . Assuming tectonic release is mainly in the horizontal plane and contributes little to  $M_{zz}$  compared to explosion and damage sources, then

$$z(K) = \frac{M_t}{M_d} \cdot (K - 1) \quad \text{and} \quad zM_d = M_t \cdot (K - 1), \quad (5)$$

which makes use of equation 6 in PT11. The net volumetric moment  $M_I$  equals  $M_t \cdot (K+2)/3$ . When  $K = 1$ , the moment of the dipole source is zero, and  $M_I = M_t$ . For  $K > 1$ ,  $zM_d > 0$ , and  $M_I > M_t$ ; meanwhile if  $K < 1$ ,  $zM_d < 0$ , and  $M_I < M_t$ . Thus,  $M_I$  exceeds the moment due to cavity formation if the value of source parameter  $K$  is greater than one.

Predictions of  $M_t$  were made by PT11 for comparison with  $M_I$  estimates of Pahute Mesa explosions. The results showed that  $M_I > M_t$  for explosions with  $K > 1$ , consistent with an additional source of volumetric moment due to damage. To quantify how much additional moment was present, PT11 adopted a power-law model of the form,  $M_I = M_t \cdot K^x$ , and attempted to estimate the exponent  $x$ . Unfortunately,  $M_I/M_t$  ratio observations show too much scatter to allow a very reliable determination of  $x$ . Due to the importance of quantifying the excess moment and testing observations against the model,  $M_I = M_t \cdot (K+2)/3$ , additional work has been carried out using  $M_s$  yield scaling observations for Pahute Mesa explosions with ground-truth yields to constrain the range of acceptable  $x$  values more tightly than  $M_I/M_t$  observations were able to.

### Constraints on $x$ from $M_s$ Yield Scaling Observations

The Rayleigh-wave reduced excitation spectrum  $A(\omega)$  is a measure of the azimuth-independent radiation of the seismic source (Patton, 1988). It is extracted from a linear decomposition of path-corrected complex amplitudes (real and imaginary parts) for a station network into five constituent azimuthal radiation patterns (1,  $\cos\theta$ ,  $\sin\theta$ ,  $\cos 2\theta$ ,  $\sin 2\theta$ ; Romanowicz, 1982). The  $A$  spectrum is related to the strength and polarity of the constant term. For long-periods  $T$  ( $T = 2\pi/\omega$ ,  $\omega$  is angular frequency), the  $A$  spectrum can be written in terms of Rayleigh-wave excitation and source parameters for the model under development (Patton and Taylor 2008, hereafter PT08)

$$A(\omega) \equiv f(K) \cdot M_I \cdot G_1(\omega), \quad (6)$$

where  $G_1(\omega)$  is a Green's function and  $f(K) = (6-2K)/(2+K)$ . Using the DJ91 scaling model,  $M_t$  can be expressed as

$$M_t = \Lambda \cdot \rho^{0.21} \cdot \alpha^{0.85} \cdot h^{-0.79} \cdot W, \quad (7)$$

where  $h$  is depth of burial, and  $\Lambda$  is a constant of proportionality. Using the power law model  $M_I = M_t \cdot K^x$ , then

$$A(\omega) = \Lambda \cdot f(K) \cdot K^x \cdot \Omega \cdot W \cdot G_1(\omega) , \quad (8)$$

where  $\Omega = \Omega(h) = \rho^{0.21} \cdot \alpha^{0.85} \cdot h^{-0.79}$  and  $\rho = \rho(h)$ ,  $\alpha = \alpha(h)$ . PT08 developed an empirical template  $A_t(\omega)$  for A spectra using an ensemble of Pahute Mesa explosions. The gain  $A'_i$  is a multiplicative scaling factor applied to the template to match the A-spectrum amplitude of the  $i$ th explosion. Between 0.1 and  $\sim 0.025$  Hz, the template matches the frequency dependence of  $G_1$  computed for a Pahute Mesa velocity model. The model predicts little variation of  $G_1$  for burial depths between 500 and 1500 m. Thus,  $A_t(\omega) \approx \gamma \cdot G_1(\omega)$  and  $A_i(\omega) \approx A'_i \cdot \gamma \cdot G_1(\omega)$ , where  $\gamma$  is an event-independent scaling factor with physical units of moment in Nm. Substituting for  $A(\omega)$  into equation (8), the gain factor  $A'_i$  for the  $i$ th explosion is

$$A'_i \approx \Lambda' \cdot f(K_i) \cdot K_i^x \cdot \Omega_i \cdot W_i , \quad (9)$$

where  $\Lambda'$  ( $= \Lambda/\gamma$ ) is independent of yield. I will establish empirically that  $\log[A']$  and network  $M_s$  scale one-to-one for nuclear explosions detonated on Pahute Mesa. This scaling equivalence will allow  $M_s$ -yield scaling to be interpreted with the new explosion source model since

$$M_{si} \sim \zeta \log[W_i] \sim \log[f(K_i)] + x \log[K_i] + \log[\Omega_i] + \log[W_i] , \quad (10)$$

where  $\zeta$  is the apparent yield scaling exponent observed for  $M_s$ . Density and  $P$  wave speed of the source medium (and hence  $\Omega$ ) vary with burial depth, and therefore with yield for a containment practice, such as  $h_i \sim 120 \cdot W_i^{1/3}$ . Since  $K$  shows a systematic dependence on yield (PT11), all terms on the right-hand side of equation (10) will be expressed with a power-law dependence as follows

$$K_i \sim W_i^a , \quad (11)$$

$$f(K_i) = \frac{6 - 2K_i}{2 + K_i} \sim W_i^b , \text{ and} \quad (12)$$

$$\Omega_i = \rho_i^{0.21} \cdot \alpha_i^{0.85} \cdot h_i^{-0.79} \sim W_i^c , \quad (13)$$

where exponents  $a$ ,  $b$ ,  $c$  and  $\zeta$  will be estimated from measurements or, in the case of  $\Omega_i$ , from a velocity model and cube-root containment rule. The yield exponent  $\zeta$  is related to the other exponents as follows

$$\zeta = ax + b + c + 1 , \quad (14)$$

and solving for  $x$

$$x = \frac{(\zeta - 1) - (b + c)}{a} . \quad (15)$$

Values of  $x$  consistent with observed yield scaling of  $M_s$  for Pahute Mesa explosions will be found, but first the scaling equivalence of network  $M_s$  and  $\log[A']$  must be shown.

### Scaling Equivalence of $M_s$ and $\log[A']$ and Yield Scaling Analysis

Figure 1 displays plots of  $\log[A']$  against  $M_s$  for five different published data sets. All network  $M_s$  determinations, with the exception of  $M_s$  reported by Selby et al. (2011), scale one-to-one with  $\log[A']$ . An average network  $M_s$  was computed using Jih and Baumstark (1994)  $M_s$  values to normalize the baseline offsets seen in Figure 1 (a-d). The average  $M_s$  plotted against  $\log[A']$  has a slope of 1.00 and a  $1-\sigma$  formal error from regression analysis of  $\pm 0.03$ .

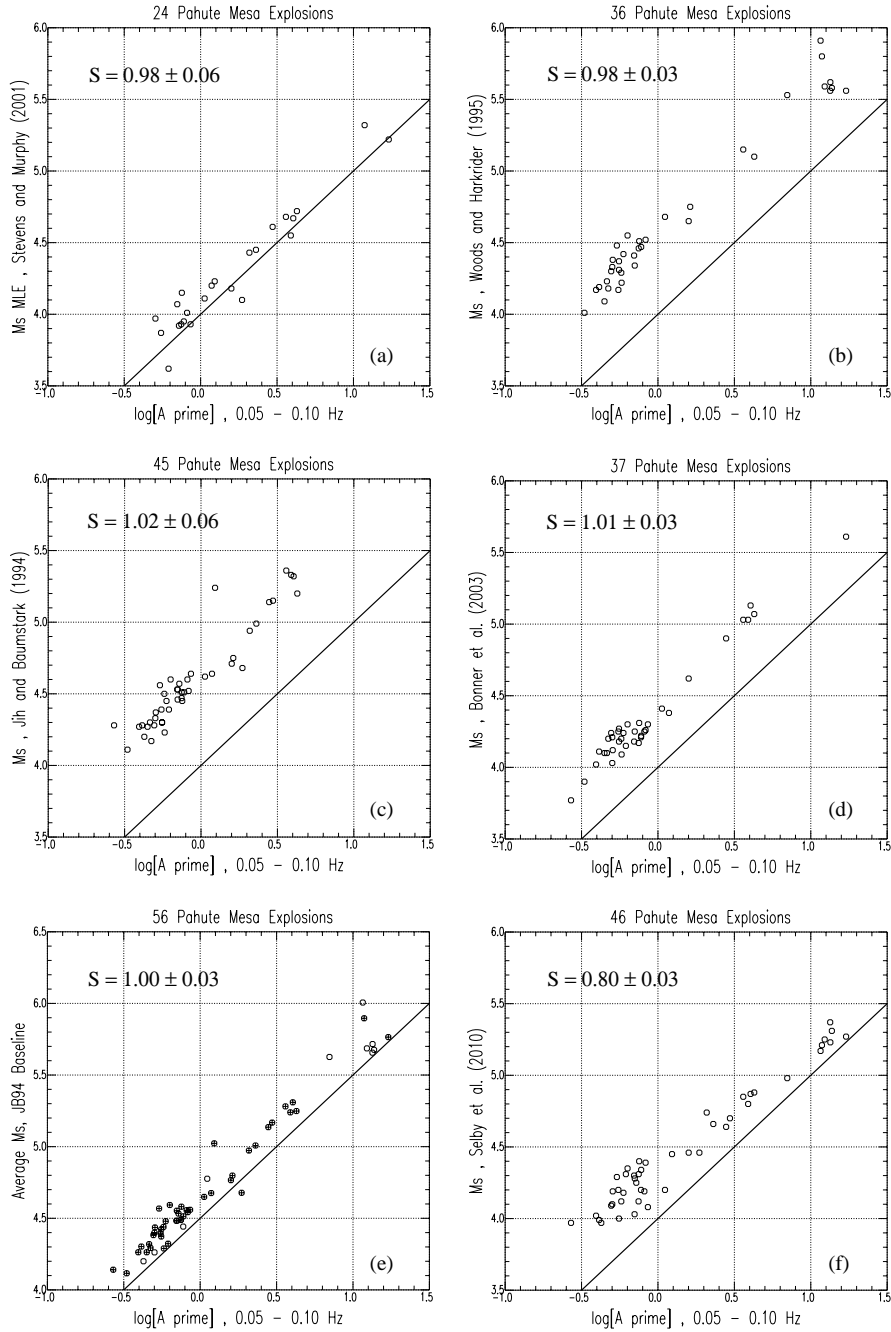


**Figure 1. Plots of various network  $M_s$  data sets against  $\log[A']$  for Pahute Mesa explosions.**  $M_s$  data sets are taken from (a) Stevens and Murphy (2001), (b) Woods and Harkrider (1995), (c) Jih and Baumstark (1994), (d) Bonner et al. (2003), and (f) Selby et al. (2011). Average network  $M_s$  are based on the first four data sets with a baseline established arbitrarily by Jih and Baumstark. Open circles in (e) are explosions with only one data set reporting a network  $M_s$ ; closed circles have multiple data sets reporting.

Note a change in vertical scale in Figure 1e, and the arbitrary shift in the line with a slope of 1 to facilitate comparison to the data. Average  $M_s$  are available for 76 Pahute Mesa explosions. In addition,  $M_s$  values were available for 56 explosions by converting  $\log[A']$  measurements to equivalent  $M_s$  values by adding a constant offset of 4.655 magnitude units (mu) determined from the data plotted in Figure 1e.

In order to mitigate effects of the water table on the results, the yield-scaling analysis was restricted to explosions below the nominal standing water level on Pahute Mesa (640 m). Thirty-four explosions meet this restriction, Kash with the shallowest burial depth (645 m) and Muenster the deepest (1452 m). Rex, a high-leverage, overburied shot with an announced yield of 19 kt and burial depth of 671 (Springer et al., 2002;  $\sim 250 \text{ m}/\text{kt}^{1/3}$ ), was omitted from the analysis, bringing the total down to 33. Of those 33 shots, 27 have  $K$  values and 25 have inferred  $M_s$  from  $\log[A']$ .

Three coupling scenarios are considered: (1) no coupling variations with burial depth (DOB; uniform coupling), (2) coupling appropriate for  $P$  waves based on assessments of Murphy (1996), and (3) coupling based on a sigmoid curve fit  $\Sigma(h)$  to surface wave observations (PT11).

According to Murphy (1996, p. 225), "...for explosions in dry, porous media, such as dry alluvium or tuff, ... the average  $m_b$  values for a given yield are lower than those in hard rock by about  $0.50 \pm 0.25 \text{ mu}$ ."

Coupling variations for  $P$  waves were based on the same sigmoid curve used for surface waves, but adopting 0.5 mu for the shallow-depth asymptote (coupling factor of  $10^{-0.5} = 0.32$ ). The shallow-depth asymptote of  $\Sigma(h)$  has a coupling factor of  $\sim 0.04$ . Coupling curves for  $P$

and surface waves, plotted in Figure 2, differ by about a factor of two at a burial depth of 640 m.  $P$  wave coupling factors weight the down-going rays more heavily than do surface waves which require a free surface for their existence. Down-going rays encounter water-saturated media where coupling improves, while surface waves sample the integrated effects of rays leaving at all take-off angles. As such, one might expect surface wave coupling factors to be smaller than their  $P$  wave counterparts for Nevada National Security Site (NNSS, formerly the Nevada Test Site NTS) media.

Estimates of model parameters for linear regressions involving official yields are provided in Tables 1 through 3. Table 1 lists estimates of the yield scaling exponent  $\zeta$ . Results are provided for the combined data sets of average  $M_s$  and inferred  $M_s$ , a total of 58 measurements, as well as data sets of just 33 average  $M_s$  measurements and 25 inferred  $M_s$  from  $\log[A']$ . While the results are consistent across all three data sets, systematic variations in estimates of  $\zeta$  for the different coupling scenarios are found as expected. The scaling exponents for surface wave coupling are smaller than their counterparts for  $P$  wave coupling which in turn are smaller than for uniform coupling.

**Table 1:  $M_s$ - $\log[W]$  Scaling for Three Coupling Scenarios, Pahute Mesa**

Data set	Uniform	$P$ wave	Surface wave
58 measurements 33 with $M_s$ 25 with $\log[A']$	$\zeta = 1.144 \pm 0.036$ $\sigma = 0.111$ CC = 0.97	$\zeta = 1.039 \pm 0.035$ $\sigma = 0.107$ CC = 0.97	$\zeta = 0.853 \pm 0.038$ $\sigma = 0.118$ CC = 0.95
33 shots with $M_s$ $h > 640 \text{ m}$	$\zeta = 1.143 \pm 0.052$ $\sigma = 0.123$	$\zeta = 1.039 \pm 0.049$ $\sigma = 0.115$	$\zeta = 0.850 \pm 0.051$ $\sigma = 0.120$
25 shots with $\log[A']$ $h > 640 \text{ m}$	$\zeta = 1.148 \pm 0.049$ $\sigma = 0.098$	$\zeta = 1.046 \pm 0.050$ $\sigma = 0.100$	$\zeta = 0.860 \pm 0.059$ $\sigma = 0.118$

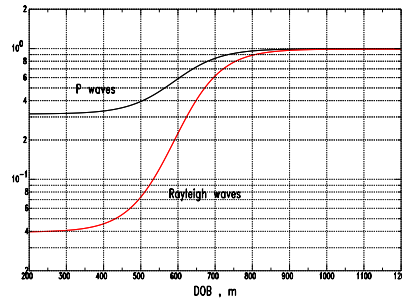


**Figure 2. Coupling factors for  $P$  waves (black) and Rayleigh waves (red).**

Table 2 summarizes scaling results for  $K$ ,  $f(K)$ , and  $\Omega(h)$ . The dependence of  $\Omega(h)$  on yield was obtained for a cube-root containment practice using layered models based on studies of Earth structure on Pahute Mesa by Ferguson et al (1994) and Leonard and Johnson (1987). Estimates of density and  $P$ -wave speed appropriate for surface wave excitation were obtained using a method that averages material properties over the elastic radius (see PT11).

**Table 2: Yield Regressions on  $K$ ,  $f(K)$ , and  $\Omega(h)$** 

$K$	$f(K)$	$\Omega(h)$
$n = 27, h > 640 \text{ m}$ $a = -0.291 \pm 0.044$ $\sigma = 0.092$ $\text{CC} = 0.80$	$n = 27, h > 640 \text{ m}$ $b = 0.262 \pm 0.046$ $\sigma = 0.096$ $\text{CC} = 0.76$	$n = 33, h > 640 \text{ m}$ $c = -0.151 \pm 0.011$ $\sigma = 0.025$ $\text{CC} = 0.93$
$n \equiv \text{number of explosions}; a, b, c \equiv \text{scaling slopes}; \sigma \equiv \text{standard deviation of residuals}; \text{CC} \equiv \text{data correlation}$		

With estimates of scaling slopes  $\zeta$ ,  $a$ ,  $b$ , and  $c$  so obtained, equation (15) can be used to compute values of  $x$ , the exponent on  $K$ . The results are provided in Table 3. While  $x$  does not show variation between different data sets due to consistent  $M_s$ -yield scaling rates  $\zeta$  in Table 1, there are significant variations for the three coupling scenarios. Uniform coupling, which we know is not appropriate for any test area at NNSS, has a small and slightly negative exponent. Coupling scenarios based on  $P$  wave and surface wave estimates (Figure 2) have positive exponents consistent with surplus volumetric moment above and beyond what cavity formation predicts. Based on surface wave coupling,  $M_s$  yield scaling favors an exponent of  $\sim 1$ . If surface wave coupling factors are biased for some reason, the exponent might be as small as 0.2 based on  $P$  wave coupling, but such coupling for surface waves seems unlikely for reasons stated above. Thus,  $M_s$  scaling results presented herein bound the exponent on  $K$  to be greater than 0.2 but perhaps less than 0.9. This range is significantly smaller than that suggested by  $M_I/M_t$  observations ( $x > 1$ ; PT11).

**Table 3: Estimation of Scaling Exponent  $x$** 

Data set	Uniform		$P$ wave		Surface wave	
	$\zeta$	$x$	$\zeta$	$x$	$\zeta$	$x$
58 measurements	1.14	-0.1	1.04	+0.2	0.85	+0.9
33 shots with $M_s$	1.14	-0.1	1.04	+0.2	0.85	+0.9
25 shots with $\log[A']$	1.15	-0.1	1.05	+0.2	0.86	+0.9
$x = [(\zeta - 1) - (b + c)] / a$ ; estimates of $a$ , $b$ , and $c$ provided in Table 3						

As shown in the previous section, the source model predicts the following relationship between net volumetric moment  $M_I$  and moment due to cavity formation  $M_t$

$$M_I = M_t \cdot \left( \frac{K+2}{3} \right). \quad (16)$$

For  $1 < K < 2.5$ , where 2.5 is the upper limit measured for Pahute Mesa explosions, the function  $(K+2)/3$  is best fit by the power-law model,  $0.977 \cdot K^{0.453}$ . Thus bounds on  $x$  ( $0.2 < x < 0.9$ ) estimated from  $M_s$  yield scaling observations are consistent with the source model prediction (0.453).  $K$  values of 1.5, 2.0, and 2.5 predict net volumetric moment  $M_I$  exceeds cavity formation moment  $M_t$  by  $\sim 17$ , 33, and 50%, respectively, due to damage of the source medium. A back-of-the-envelope calculation for a 100-kt explosion with  $K$  value of 2 translates a 33% moment increase into  $\sim 0.1\%$  volumetric dilation of damaged source medium confined to an inverted cone extending from the cavity formed by the explosion to the free surface and an circular area around ground zero where spallation is strongest ( $\sim 160$  scaled meters).

### Inferences of Material Properties and $m_b$ Bias of the North Korean Test Site.

Even with complete understanding of explosion source mechanisms, accurate yield estimation still requires reliable knowledge of source medium velocity structure and near-source propagation effects. For new test sites in remote, seismic-inactive areas, such knowledge can be difficult to obtain, requiring extensive data collection efforts and painstaking observational work that can take years before producing reliable results. The North Korean (NK) test site is a prime example of just this scenario where little is known about the material properties of the source region and the efficiency of wave propagation under the northern Korean Peninsula.

In this section, I will show how source theory can be exploited to make inferences about source medium wave speeds and  $m_b$  bias for the NK test site using (1) yield : depth-of-burial tradeoff curves ( $W:h$  TOCs) and (2)  $\{m_b - M_s\}$  double differences between the 2009 NK test and explosions conducted at NNSS. Herein  $W:h$  TOCs based on measurements of  $m_b$  and  $M_I$  are presented for the 2009 test. A fundamental assumption made to derive TOCs is that the test can be approximated by a pure explosion source. Measurements of  $m_b$ ,  $M_s$ , and the results of moment tensor inversions suggest that the sources of both NK tests are nearly pure explosions with relatively minor energy radiated at long periods from tectonic release and source medium damage (e.g., Ford et al., 2009; Shin et al., 2010; PT08, PT11). Sharpe's (1942) theory will be used to relate seismic radiation to the reduced displacement potential  $\psi(\tau)$  where  $\tau$  is reduced time  $t - r/\alpha$ ,  $r$  is radial distance, and  $\alpha$  is the speed of  $P$  waves in the medium. I make use of two well-known scaling models, one due to HA67 (used by MM71) and the other due to DJ91. These models predict different TOCs. The material presented in this section is abstracted from Patton (2011).

Figure 3 shows  $W:h$  TOCs for the 2009 NK test based on measurements of  $m_b$  and  $M_I$  from Selby et al. (2011). Assumed material property values for the NK test site are those adopted by Koper et al. (2008; hereafter KHB08):  $\rho_{NK} = 2500 \text{ kg/m}^3$ ,  $\alpha_{NK} = 5100 \text{ m/s}$ ,  $v_{NK}$  (Poisson ratio) = 0.2354, and  $GP_{NK}$  (gas porosity) = 0.5%. The test site bias  $\delta_{NK}$  was assumed to be zero. Of interest are the offsets between  $\text{TOC}(m_b)$  and  $\text{TOC}(M_I)$  for both scaling models, where  $\text{TOC}(M_I) > \text{TOC}(m_b)$ . Not only are the offsets significant, but so are the predictions of the depth dependence of yield. Important questions to answer are: (1) what causes the offsets, and (2) which set of TOCs, HA67 or DJ91, is a better

representation of the truth. This study addresses the first question. I assert that the offsets are caused by systematic errors due to inaccurate medium parameters and  $m_b$  bias adopted for the computation of TOCs in Figure 3. Measurement errors in  $m_b$  and  $M_I$  are assumed to be second order compared to systematic errors. As such, offsets provide constraints on medium properties and  $\delta_{NK}$ . Two constraint equations involving  $\alpha_{NK}$ ,  $v_{NK}$ , and  $\delta_{NK}$  will be derived from the TOCs and from  $\{m_b - M_s\}$  double differences between the 2009 NK test and calibration explosions

detonated on Pahute Mesa.  $\{m_b - M_s\}$  double differences between the 2009 test and NNSS explosions constrain a three-dimensional surface relating free parameters  $\alpha_{NK}$ ,  $v_{NK}$ , and  $\delta_{NK}$ . A fourth dimension of parameter space,  $\rho_{NK}$ , was eliminated by the use of a  $\rho-\alpha$  relationship. NNSS serves as a reference test site where material properties  $\alpha_{NNSS}$ ,  $v_{NNSS}$  and test site bias  $\delta_{NNSS}$  are calibrated, and the explosion sources are well-quantified. NNSS sources must also be pure explosions to the first degree, as the NK explosions are. Two selection criteria were used: (1)  $m_b > 5.8$  and (2)  $h > \sim 750 \text{ m}$ . PT11 found that large Pahute Mesa explosions meeting these criteria have measured  $M_I$  that are consistent with the predictions of classical moment  $M_t$  based on cavity formation alone. Twenty explosions met these criteria.

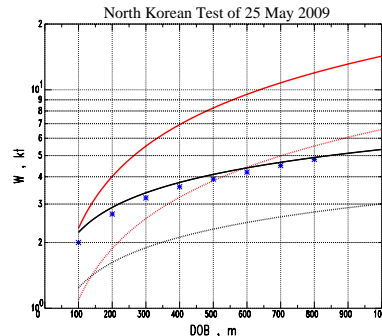


**Figure 3.  $W:h$  TOCs for the 2009 NK test.**  
Two sets are shown: black curves based on HA67 scaling and red curves for DJ91 scaling. Solid lines are  $\text{TOC}(M_I)$ s, dotted lines are  $\text{TOC}(m_b)$ . \* symbols indicate  $\text{TOC}$  obtained by Murphy et al. (2010) from modeling regional  $P$  wave source spectra.

An expression for  $\{m_b - M_s\}$  double differences between tests conducted at the NK test site and NNSS is

$$\begin{aligned} \{m_b - M_s\}_{\text{NK}} - \{m_b - M_s\}_{\text{NNSS}} = \\ -\frac{1}{2} \left( \log \left[ \frac{\rho_{\text{NK}}}{\rho_{\text{NNSS}}} \right] + 1.3 \log \left[ \frac{\zeta_{\text{NK}}}{\zeta_{\text{NNSS}}} \right] + 1.6 \log \left[ \frac{\alpha_{\text{NK}}}{\alpha_{\text{NNSS}}} \right] \right) + \log \left[ \frac{\psi_{\text{NK},1}}{\psi_{\text{NK},2}} \cdot \frac{\psi_{\text{NNSS},2}}{\psi_{\text{NNSS},1}} \right] - \delta_{\text{NK}} + \delta_{\text{NNSS}}, \end{aligned} \quad (17)$$

(see Patton, 2011).  $\psi_{\text{NK},1}$  is shorthand for  $\psi_{\text{NK}}(\omega_1)$ , and  $\zeta = (\beta/\alpha)^2$ .  $\omega_1$  and  $\omega_2$  are frequencies where  $m_b$  and  $M_s$  are measured. Equation (17) involves  $m_b$  biases for both test sites.  $\delta_{\text{NNSS}}$  was estimated from  $m_b(P) - m_b(Lg)$  residuals for the 20 calibration shots ( $-0.27 \pm 0.02$  mu). Ratios  $\psi_{\text{NNSS},1} / \psi_{\text{NNSS},2}$  were measured on potentials computed with the MM71 model. Since HA67 and DJ91 predict similar cavity radii for standard burial practice, the ratios were not affected by the choice of scaling model. Ratios  $\psi_{\text{NK},1} / \psi_{\text{NK},2}$  were measured for six realizations of MM71 spectra for granite explosions with yields 3, 6, and 12 kt and two NK velocity models, one with  $\alpha_{\text{NK}}$  of 5100 m/s and one with 5600 m/s. The average log ratios for the two velocity models are 0.10 and 0.06 mu, respectively. For NK models, spectra were computed for a scaled burial depth of 250 m/kt<sup>1/3</sup>. As such, the DJ91 model predicts smaller cavity radii than HA67, hence higher corner frequencies and smaller ratios. I adopted a value of 0.06 mu for  $\log[\psi_{\text{NK},1} / \psi_{\text{NK},2}]$ , which is 0.1 mu smaller than  $\log[\psi_{\text{NNSS},1} / \psi_{\text{NNSS},2}]$ .  $\{m_b - M_s\}_{\text{NK}}$  equals 1.04 mu and the mean  $\{m_b - M_s\}_{\text{NNSS}}$  for 20 Pahute Mesa explosions is  $1.19 \pm 0.04$  mu. After making substitutions, equation (17) reduces to

$$1.3 \log \left[ \frac{\zeta_{\text{NK}}}{\zeta_{\text{NNSS}}} \right] + 2.13 \log \left[ \frac{\alpha_{\text{NK}}}{\alpha_{\text{NNSS}}} \right] = 0.64 - 2\delta_{\text{NK}}. \quad (18)$$

Using appropriate values for  $\zeta_{\text{NNSS}}$  and  $\alpha_{\text{NNSS}}$ ,  $\zeta_{\text{NNSS}}^{1.3} \cdot \alpha_{\text{NNSS}}^{2.13} = 7.37 \times 10^6$ . Solving for  $\alpha_{\text{NK}}$ , a three-dimensional surface is obtained

$$\alpha_{\text{NK}} = 3347 \cdot 10^{-0.94\delta_{\text{NK}}} \cdot \zeta_{\text{NK}}^{-0.61}. \quad (19)$$

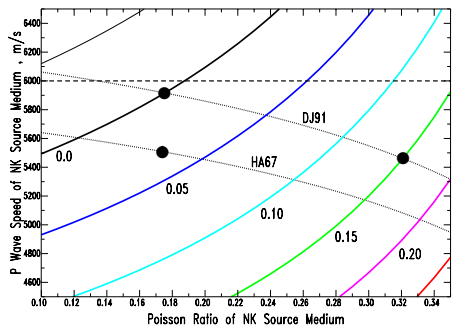


**Figure 4. Contours (black dotted lines) satisfying the constraint  $\text{TOC}(M_I) = \text{TOC}(m_b)$ .** Contours from equation (19) are plotted for selected  $\delta_{\text{NK}}$  ranging from  $-0.05$  to  $0.25$  mu in steps of  $0.05$  (thin black, heavy black, blue,..., red). A plausible upper bound on  $\alpha_{\text{NK}}$  for near-surface granite is shown by the horizontal dash line (6000 m/s).

from both scaling models are considerably faster than 5100 m/s assumed by KHB08 if  $\delta_{\text{NK}}$  is small ( $< 0.15$  mu), or under the reasonable assumption that  $v_{\text{NK}}$  for intact granite is less than 0.3.

An offset  $O_W$  is defined as a multiplicative factor such that  $\text{TOC}(M_I) = O_W \cdot \text{TOC}(m_b)$ . Equations for offsets,  $O_W(\text{HA67})$  and  $O_W(\text{DJ91})$ , lead to expressions for  $\alpha_{\text{NK}}$  which exhibit simple inverse relationships where  $\alpha_{\text{NK}}$  increases as  $\delta_{\text{NK}}$  decreases or vice-versa.

$$\begin{aligned} \alpha_{\text{NK}}(\text{HA67}) &= 5600 \cdot 10^{-0.23\delta_{\text{NK}}} \quad \text{and} \\ \alpha_{\text{NK}}(\text{DJ91}) &= 5910 \cdot 10^{-0.23\delta_{\text{NK}}}. \end{aligned} \quad (20)$$

$\alpha_{\text{NK}}(\text{DJ91})$  is 5.5% faster than  $\alpha_{\text{NK}}(\text{HA67})$ . Using equation (19), the formulas for  $\alpha_{\text{NK}}$  can be written in terms of  $\zeta_{\text{NK}}$

$$\begin{aligned} \alpha_{\text{NK}}(\text{HA67}) &= 6639 \cdot \zeta_{\text{NK}}^{0.20} \quad \text{and} \\ \alpha_{\text{NK}}(\text{DJ91}) &= 7129 \cdot \zeta_{\text{NK}}^{0.20}. \end{aligned} \quad (21)$$

These formulas are plotted in Figure 4 along with contours of constant  $m_b$  bias from equation (19).  $P$  wave speeds at the NK test site inferred

Confirmation that revised TOCs are completely consistent for the solutions in equations (20) and (21) is provided in Figure 5. Now the TOCs overlay. These TOCs bring out several important points about the solutions. The first underscores what the contours in Figure 4 revealed, that source medium  $P$  wave speeds must be high when  $\delta_{NK}$  is small. Since compliance of the medium stiffens as  $\alpha_{NK}$  and  $\rho_{NK}$  increase, the elastic response is reduced giving a smaller  $P$  wave amplitude for a given applied pressure. Thus the TOCs for zero bias predict larger yields than initial  $TOC(m_b)$ s did (compare dotted curves in Figure 3 with the curves for  $\delta_{NK} = 0$  in Figure 5). The second point is that increasing  $\delta_{NK}$  lowers the yield predicted by TOCs. A  $\delta_{NK}$  of 0.3 mu would increase the yield by about a factor of two for DJ91 scaling were it not for compensating effects of a more compliant source medium and larger cavity radius since  $\alpha_{NK}$  decreases as  $\delta_{NK}$  increases. For DJ91 scaling, TOCs decrease a factor of 1.4 for a 0.3 mu increase in  $\delta_{NK}$  (Figure 5).

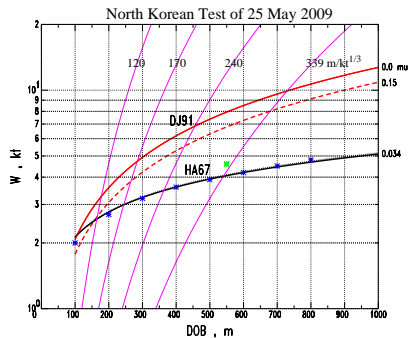


**Figure 6. Revised TOCs for 2009 NK test.**  
**TOC for HA67 scaling (black)** compares well with Murphy et al.'s TOC shown by \* symbols on the graph, and final yield, DOB shown by \* symbol. Plotted in red are "end member" solutions for DJ91 scaling with minimum and maximum  $\delta_{NK}$  (solid and dash lines). Magenta lines are for constant scaled depth of burial (e.g. 120, 169.7, 240, 339.4  $m/kt^{1/3}$ ).

## CONCLUSIONS AND RECOMMENDATIONS

This project advances new explosion source models by accounting for the effects of source medium damage on radiated  $P$ ,  $S$  and Rayleigh wave fields. Volumetric moment due to damage has been quantified. Further research is needed to test models against observed  $P/S$  ratio spectral modulations in the 0.5-3 Hz band and high-frequency yield scaling. To do so, the next step will build suitable time histories and depth distributions for damage moment-rate functions. Both time history and moment will depend on depth. A method exploiting new insights into the explosion source led to constraints on material properties for the NK test site and estimates of yield for the 2009 NK test.

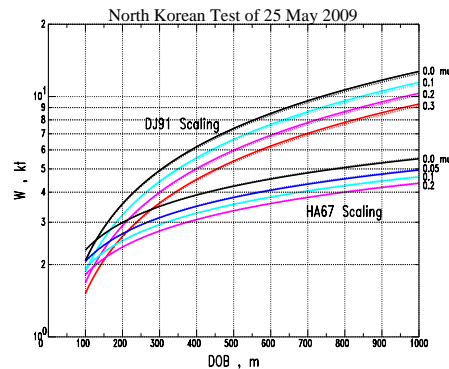


**Figure 5. W:h TOCs for a range of  $\delta_{NK}$  values.**  
 $TOC(M_f)$  and  $TOC(m_b)$ , plotted with solid and dotted lines, overlay as they should.  $\delta_{NK}$  values are: black, blue, cyan, magenta, and red for 0.0, 0.05 (HA67 only), 0.1, 0.2, and 0.3 mu (DJ91 only), respectively.

Revised  $W:h$  TOCs are plotted in Figure 6 for the solutions indicated with large black dots in Figure 4. TOCs computed using HA67 scaling for  $\delta_{NK}$ ,  $\alpha_{NK}$ ,  $v_{NK}$  of 0.034 mu, 5500 m/s, and 0.174 are consistent with the TOC of Murphy et al. (2010). Final estimates of yield and depth of burial reported by Murphy et al. are 4.6 kt and 550 m. Two solutions for DJ91 scaling, one for zero bias and one for what I believe is an upper bound, 0.15 mu, are plotted. These solutions have  $\alpha_{NK}$  of 5910 and 5450 m/s, and  $v_{NK}$  of 0.178 and 0.323, respectively, and bracket a plausible range of TOCs. Lines of constant scaled depth of burial are also plotted, showing graphically that scaled burial depths vary along the TOCs from  $\sim 80 m/kt^{1/3}$  to more than  $500 m/kt^{1/3}$  for the range of burial depths plotted. It is apparent from these results that the choice of scaling model is quite important for accurate yield estimation once explosions become over-buried. Hydrodynamic simulations for competent granite from the study of Rougier et al. (2011) favor DJ91 scaling and provide estimates of a lower bound on yield and depth of burial. For the 2009 NK test, these estimates are 5 to 6 kt and  $\sim 380$  m. At 550 m, the depth favored by Murphy et al. (2010), the yield from this study is 7 to 8 kt.

**REFERENCES**

Ben-Zion, Y. and Ampuero, J.-P. (2009). Seismic radiation from regions sustaining material damage, *Geophys. J. Int.* 178: 1351–1356, doi: 10.1111/j.1365-246X.2009.04285.x.

Bonner, J. L., D. G. Harkrider, E. T. Herrin, R. H. Shumway, S. A. Russell, and I. M. Tibuleac (2003). Evaluation of short-period, near-regional  $M_s$  scales for the Nevada Test Site, *Bull. Seismol. Soc. Am.*, 93: 1773–1791.

Denny, M. D. and L. R. Johnson (1991). The explosion seismic source function: Models and scaling laws reviewed, in *Explosion Source Phenomenology*, AGU Monograph, 65: edited by S. Taylor et al., 1–24.

Ferguson, J. F., A. H. Cogbill, and R. G. Warren (1994). A geophysical-geological transect of the Silent Canyon caldera complex, Pahute Mesa, Nevada, *J. Geophys. Res.* 99: 4323–4339.

Ford, S. R., D. S. Dreger, and W. R. Walter (2009). Source analysis of the Memorial Day explosion, Kimchaek, North Korea, *Geophys. Res. Lett.* 36: L21304, doi:10.1029/2009GL040003.

Heard, H. C. and F. J. Ackerman (1967). Prediction of cavity radius from underground nuclear explosions (U), Lawrence Radiation Laboratory Report, UCRL-50324.

Jih, R.-S. and R. R. Baumstark (1994). Maximum-likelihood network magnitude estimates of low-yield underground explosions, TBE-4617-3/TGAL-94-02, Teledyne-Brown Engineering, Arlington, VA.

Knopoff, L. and M. J. Randall (1970). The compensated linear-vector dipole: A possible mechanism for deep earthquakes, *J. Geophys. Res.* 75: 4957–4963.

Koper, K. D., R. B. Herrmann, and H. M. Benz (2008). Overview of open seismic data from the North Korean event of 9 October 2006, *Seismol. Res. Lett.* 79: 178–185.

Leonard, M. A. and L. R. Johnson (1987). Velocity structure of Silent Canyon caldera, Nevada Test Site, *Bull. Seismol. Soc. Am.* 77: 597–613.

Murphy J. R. (1996). Types of seismic events and their source descriptions, in *Monitoring a CTBT*, edited by E. S. Husebye and A. M. Dainty, Kluwer Acad., Dordrecht, Netherlands, pp. 225–245.

Mueller, R. A. and J. R. Murphy (1971). Seismic characteristics of underground nuclear detonations, Part I. Seismic spectrum scaling, *Bull. Seismol. Soc. Am.*, 61: 1675–1692.

Murphy, J. R., B. C. Kohl, J. L. Stevens, T. J. Bennett, and H. G. Israelsson (2010). Exploitation of the IMS and other data for a comprehensive advanced analysis of the North Korean nuclear tests, SAIC Final Technical Report 10/2201, DOS Contract No. SAQMMA09C0250.

Patton, H. J. (1988). Source models of the Harzer explosion from regional observations of fundamental-mode and higher mode surface waves, *Bull. Seismol. Soc. Am.*, 78: 1133–1157.

Patton, H. J. (2011). A method to infer material properties and  $m_b$  bias of the North Korean test site using yield : depth-of-burial tradeoff curves and  $\{m_b - M_s\}$  double differences, *Bull. Seismol. Soc. Am.* 101: December.

Patton, H. J. and S. R. Taylor (2008). Effects of shock-induced tensile failure on  $m_b - M_s$  discrimination: Contrasts between historic nuclear explosions and the North Korean test of 9 October 2006, *Geophys. Res. Lett.*, 35: doi:10.1029/2008GL034211.

Patton, H. J. and S. R. Taylor (2011). The apparent explosion moment: Inferences of volumetric moment due to source medium damage by underground nuclear explosions, *J. Geophys. Res.* 116: B03310.

Romanowicz, B. A. (1982). Moment tensor inversion of long period Rayleigh waves: A new approach, *J. Geophys. Res.* 87: 5395–5407.

Rougier, E., H. J. Patton, E. E. Knight, and C. R. Bradley (2011). Constraints on burial depth and yield of the 25 May 2009 North Korean Test from hydrodynamic simulations in a granite medium, *Geophys. Res. Lett.* 38: October.

Selby, N. D., P. D. Marshall, and D. Bowers (2011).  $m_b : M_s$  event screening revisited, *Bull. Seismol. Soc. Am.* 101: August.

Sharpe, J. A. (1942). The production of elastic waves by explosion pressures. I. Theory and empirical field observations, *Geophysics* 7: 144–154.

Shin, J. S., D.-H. Sheen, and G. Kim (2010). Regional observations of the second North Korean nuclear test on 2009 May 25, *Geophys. J. Int.* 180: 243–250.

Springer, D. L., G. A. Pawloski, J. L. Ricca, R. F. Rohrer, and D. K. Smith (2002). Seismic source summary of all U. S. below-surface nuclear explosions, *Bull. Seismol. Soc. Am.*, 92: 1806–1840.

Stevens, J. L. and J. R. Murphy (2001). Yield estimation from surface-wave amplitudes, *Pure appl. geophys.* 158: 2227–2251.

Woods, B. B. and D. G. Harkrider (1995). Determining surface-wave magnitudes from regional Nevada Test Site data, *Geophys. J. Int.* 120: 474–498.